Synthesis and Characterization of Nanostructured Fast Ionic Conductor $Li_{0.30}La_{0.56}TiO_3$

Quoc Nghi Pham, Claude Bohnké, Marie-Pierre Crosnier-Lopez, and Odile Bohnké*

Laboratoire des Oxydes et Fluorures (UMR 6010 CNRS), Institut de Recherche en Ingénierie Moléculaire et Matériaux Fonctionnels (FR 2575 CNRS), Université du Maine, Avenue O. Messiaen 72085 LE MANS Cedex 9, France

Received March 13, 2006. Revised Manuscript Received June 12, 2006

The preparation of a pure and nanostructured phase of the fast lithium conductor $Li_{0.30}La_{0.56}TiO_3$ at low temperature (350 °C for 2 h) is reported for the first time. The synthesis has been carried out by the Pechini-type in-situ polymerizable method. It has been shown that the molar ratios ethylene glycol/citric acid and citric acid/metals, as well as the temperature, are crucial parameters during this synthesis. A careful control of the temperature during polyesterification allowed us to prepare the nanosized phase of oxide and to avoid the formation of thermally stable impurities. The crystallite size (20−30 nm) of the oxide has been determined by the analysis of the broadening of the powder X-ray diffraction lines. The particles size has been confirmed by transmission electron microscopy and the macroporous character of the powder has been evidenced by scanning electron microscopy.

Introduction

Nanosized materials may offer anomalous and interesting properties. This has already been observed in nanoelectronics. The size effect, which is based on the quantum-mechanical confinement effect, leads to the increase of the energy of delocalized electrons with decreasing size. Such a phenomenon has been proved to be valuable in varistors, Positive Coefficient Temperature (PCT) ceramics, or gas sensor applications. More recently, it has been pointed out that ionic transport properties may also be changed by size effect. In a series of recent papers, Maier[1] shows that "regardless of fashion and prejudice" the field of nanoionics can lead to "substantially new insights regarding fundamental issues, but also to novel technological perspectives". The importance of nanoionics to electrochemistry comes from the fact that the density of interfaces becomes very high when particle size decreases. This increase of interface density can then lead to a drastic change of both the local and the overall ionic transport properties of solids but also to storage or sensor properties of these materials. Therefore, the properties of nanostructured ionic conductors deserve to be explored extensively. In such a context, the attempt to synthesize nanostructured $Li_{0.30}La_{0.56}TiO_3$ appeared to be of great interest.

The perovskite-type lithium lanthanum titanate, $Li_{3x}La_{2/3-x}TiO_3$, is well-known to be a high lithium ionic conductor having bulk conductivity of 10^{-3} S cm^{-1} at room temperature for $x = 0.10$.[2] Because of this high ionic conductivity, these compounds (hereafter called LLTO) have been studied for long time to explore the conduction mechanism and their potential use in various applications.[3] So far, most of the LLTO compounds have been prepared from the powder mixtures of oxides and carbonates by a conventional solid-state reaction method. This method of preparation requires an extensive heat treatment (1150 °C) for a long time (24 h) with intermediate grinding to achieve complete chemical reaction. Such a high-temperature procedure leads to grain growth and to lithium loss (up to 20 mol %).[4] To overcome these disadvantages, low-temperature procedures were then considered. In this context, the span of preparation procedures is enormous. The synthesis of fine grain complex multicomponent oxide ceramics with good compositional homogeneity and high purity requires the use of a good mixing of the components at the molecular level. In an account that focuses on the synthesis and characteristics of ceramics, Kakihana et al. illustrated the advantages of the Pechini-type in-situ polymerizable method over other solution techniques to prepare pure and homogeneous oxides.[5] This procedure is based on the formation of polyesters obtained from metal-chelated citric acid and polyhydroxyl alcohol.[6] The chelation process is based on the mixture of cations (M) precursor solution in an aqueous citric acid (CA) solution. These chelates undergo polyesterification when heated with ethylene glycol (EG). The reaction which is carried out in ambient atmosphere leads to metallic-citrate polyester. Heating of the polymer causes its decomposition and the

* Author to whom correspondence should be addressed. Tel: +33-2-4383-3354; fax: +33-2-4383-3506; e-mail: odile.bohnke@univ-lemans.fr.

(1) (a) Maier, J. *Solid State Ionics* **2002**, *154*−*155*, 291. (b) Maier, J. *Solid State Ionics* **2003**, *157*, 327. (c) Maier, J. *Solid State Ionics* **2002**, *148*, 367. (d) Maier, J. *Nat. Mater.* **2005**, *4*, 805.

(2) (a) Belous, A.G.; Butko, V. I.; Novitskaya, G. N.; Polianetskaya, S. V.; Khomenko, B. S.; Poplavko, Y. M. *Ukr. Fiz. Zh.* **1986**, *31*, 4, 576. (b) Inaguma, Y.; Liquan, C.; Itoh, M.; Nakamura, T.; Uchida, T.; Ikuta, H.; Wakihara, M. *Solid State Commun.* **1993**, *86*, 10, 689.

(3) (a) Stramare, S.; Thangadurai, V.; Weppner, W. *Chem. Mater.* **2003**, *15*, 3974 and references therein. (b) Bohnke, O.; Emery, J.; Fourquet, J.-L.; Badot, J.-C. *Recent Research Developments in Solid State Ionics*; Edt S. G. Pandalai; Transworld Research Network, 2003; Vol. 1 and references therein.

(4) (a) Inaguma, Y.; Chen, L.; Itoh, M.; Nakamura, T. *Solid State Ionics* **1994**, *70/71*, 196. (b) Emery, J.; Buzaré, J−Y.; Bohnke, O.; Fourquet, J.-L. *Solid State Ionics* **1997**, *99*, 41.

(5) Kakihana, M.; Yoshimura, M. *Bull. Chem. Soc. Jpn* **1999**, *72*, 1427.

(6) Pechini, M. P. U.S. Patent 3,330,697, 1967.

10.1021/cm060605f CCC: $33.50
Published on Web 08/04/2006

formation of a powder precursor by pyrolysis. Further appropriate heat treatments yield a fine oxide powder.

In the present study, we will describe the polymerizable precursor method that we used. We will particularly emphasize the role of the two EG/CA and CA/M molar ratios as well as the pyrolysis temperature as crucial parameters during the synthesis to prepare the nanosized phase of LLTO and to avoid the formation of impurities. Herein, we demonstrate, for the first time, that the synthesis of pure LLTO is possible at low temperature. The study of the crystallite size of LLTO was carried out by the analysis of the broadening of the X-ray diffraction (XRD) lines. The size of the crystallites thus obtained was confirmed by transmission electron microscopy (TEM). Furthermore, the macroporous character of the powder has been evidenced by scanning electron microscopy (SEM).

Experimental Section

For the synthesis of $Li_{0.30}La_{0.56}TiO_3$, Ti fine powder (99%, 325 mesh) from Alfa Aesar, Li_2CO_3 (99.997%) from Aldrich, and La_2O_3 (99.999%) from Rhone-Poulenc were used as starting materials. The titanium solution was prepared by dissolution of Ti powder with hydrogen peroxide (30%) from Carlo Erba and ammonia (35%) from Fischer Scientific. Lithium carbonate and lanthanum oxide were dissolved in nitric acid from extra pure HNO_3 (65%) from Riedel de Haën. The polymer precursor was prepared from the above solutions with CA (99.5%) and EG (99%) from Aldrich. The detailed procedure of the synthesis is given in the next part of the paper.

Thermal analysis (TGA) was performed with a Setaram TGD-TA92 equipment at a heating rate of 5 °C min^{-1} in air using Pt crucibles.

Powder XRD patterns have been recorded at room temperature with a Philips X'Pert PRO diffractometer (Cu Kα radiation), equipped with a linear X'Cellerator detector, in the 2θ range from 5 to 70° with an interpolated step of 0.08°. For the structural and microstructural analysis, slow scan patterns were recorded at room temperature in the 2θ range from 8 to 120° with an increment step of 0.0167° and a total collecting time of 7 h 33 min. The fluoride $Na_2Ca_3Al_2F_{14}$ (NAC)[7] was used as an instrument standard (std) for determining the instrumental broadening. The mean coherence length (L) was calculated using the Scherrer formula:[8]

$$L = \frac{K\lambda}{\beta \cos(\theta)} \tag{1}$$

where β is interpreted as a volume-averaged crystallite dimension perpendicular to the reflecting planes (intrinsic peak width in radians), θ is the diffraction angle, λ is the X-ray wavelength, and K is the Scherrer constant that depends on the crystallite shape ($K = 0.94$ for spherical crystallites[9]). It was the first model, and the simplest approach, established on size broadening and later on generalized to estimate grain size by XRD. The β value is obtained by fitting some Bragg peaks using the WinFit software.

Besides, the Rietveld method[10] using the X'Pert HighScore Plus program (PANalytical, Almelo, The Netherlands) was used for the microstructural refinement with a peak shape described by a pseudo-Voigt function. The width and shape of a diffraction peak are a convolution of both the instrumental broadening and the broadening arising from the sample. The crystallite size (L) and microstrain (e) were described by the following relationships:

$$L = \left(\frac{180}{\pi}\right)\frac{\lambda}{(W - W_{std})^{0.5}} \tag{2}$$

$$e = \frac{[(U - U_{std}) - (W - W_{std})]^{0.5}}{\frac{1}{100}\left(\frac{180}{\pi}\right)4(2 \ln 2)^{0.5}} \tag{3}$$

The U parameter contains the information about the strain broadening while the W parameter is related to the size broadening.

Microstructure observations were performed using a Hitachi 2300 SEM. Thin specimens for TEM study were obtained by ultrasonically dispersing particles in ethanol and depositing one drop of the resulting suspension on a Cu grid covered with a holey carbon film. After drying, the grid was fixed in a side-entry ± 30° double-tilt specimen holder and was introduced in a JEOL-2010 electron microscope operating at 200 kV.

Granulometry has been carried out with a Beckman Coulter equipment in water at room temperature. In-situ ultrasonic vibration has been used before measurement of the particles' size.

Results and Discussion

Synthesis of $Li_{0.30}La_{0.56}TiO_3$, Influence of the CA/M and EG/CA Molar Ratios. One of the crucial steps in the herein used modified Pechini-type method was to prepare a highly water soluble precursor to avoid the use of alkoxides, which are not stable in open air, as previously reported.[11] The formation of water-resistant peroxo-citrato-metal complex during the synthesis of LLTO, instead of alkoxides that are extremely sensitive to moisture, is of great importance for inexpensive and convenient aqueous synthesis of these ceramics for commercial applicability of these oxides. The main goal of this Pechini-type synthesis method is to obtain a polymeric network made of randomly and homogeneously distributed cations able to lead to a powder precursor by decomposition of the organic matrix.

In this work, we study the particular compound $Li_{0.30}La_{0.56}TiO_3$ which is the best conductor of the solid solution $Li_{3x}La_{2/3-x}TiO_3$. Figure 1 shows the flowchart of the synthesis procedure used to prepare this compound. For 1 g of LLTO, Ti metal powder is dissolved in aqueous solution containing 30% H_2O_2 (20 mL) and 35% ammonia solution (5 mL) at room temperature. This yields a yellowish transparent titanium peroxo solution. CA is added to the solution to form titanium-chelated citric acid. The amount of CA is a crucial parameter in the synthesis. We performed different syntheses by varying the ratio CA/M from 1 to 12 (M represents the total number of moles of cations: Li, La, and Ti). Stoichiometric amounts of high-purity La_2O_3 and Li_2CO_3 are dissolved in HNO_3 (30%). This mixture is added to the above solution. To improve the homogeneity of the metal-citrate complex, which becomes slightly reddish in

(7) Courbion, G.; Ferey, G. *J. Solid State Chem.* **1988**, *76*, 426.
(8) Scherrer, P. *Nachr. Göttingen* **1918**, *2*, 98.
(9) Klug, H. P.; Alexander, L. E. *X-ray Diffraction Procedures for Polycrystalline and Amorphous Materials*, 2nd ed.; Wiley-Interscience: New York, 1974; pp 618−687.
(10) Rietveld, H. M. *J. Appl. Crystallogr.* **1969**, *2*, 65.
(11) (a) Kakihana, M.; Szanics, J.; Tada, M. *Bull. Korean Chem. Soc.* **1999**, *20*, 8, 893. (b) Kakihana, M.; Tada, M.; Shiro, M.; Petrykin, V.; Osada, M.; Nakamura, Y. *Inorg. Chem.* **2001**, *40*, 891. (c) Vijayakumar, M.; Inaguma, Y.; Mashiko, W.; Crosnier-Lopez, M.-P.; Bohnke, C. *Chem. Mater.* **2004**, *16*, 2719.

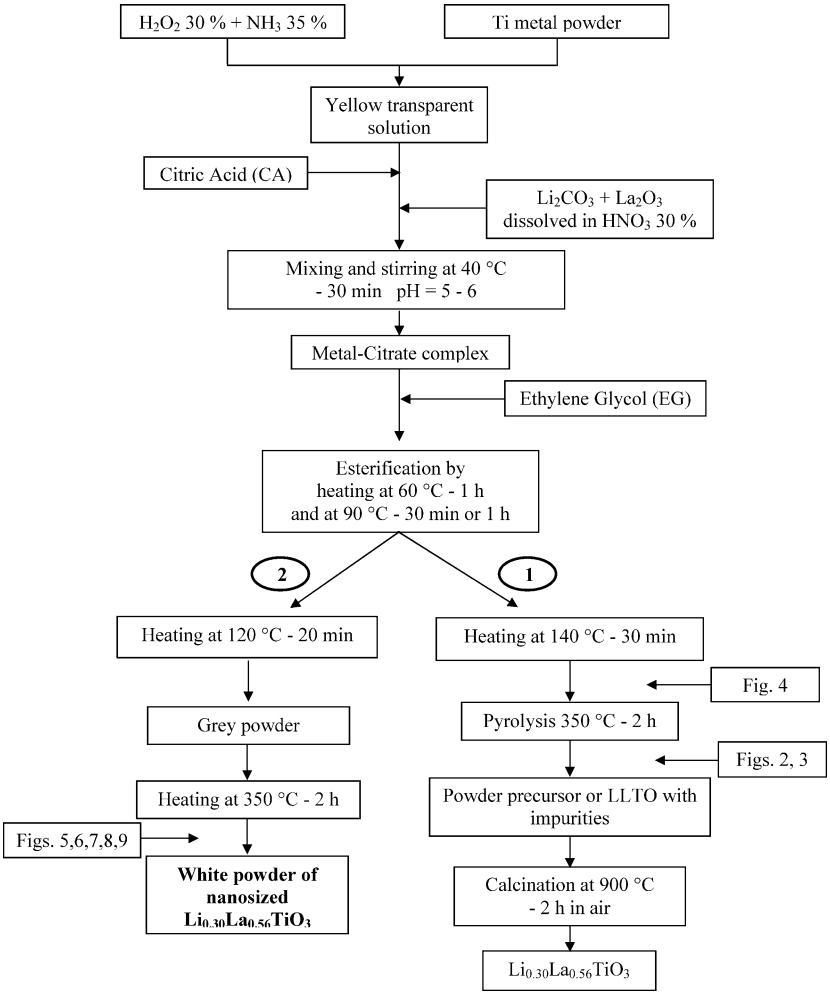

Figure 1. Flowchart for the preparation of nanosized LLTO.

color, the solution is heated in an oil bath, up to 40 °C, and is stirred for 30 min. The pH of the solution is maintained close to 5−6 by adding slowly either HNO_3 or NH_4OH. EG is then added to the above solution. The amount of EG is also a crucial parameter. Different syntheses have been carried out with different ratios of EG/CA in the range from 1 to 4. The temperature is increased to 60 °C for 1 h and then to 90 °C for 0.5 or 1 h, depending on the CA/EG ratio, to slowly evaporate water. According to Xu,[12] this step is crucial to promote esterification between the hydroxyl groups of EG and the carboxylic acid groups of CA. A very viscous solution is obtained. This solution is then heated at 140 °C for 30 min in the oil bath with magnetic stirring to ensure a better control of the temperature and a uniform temperature in the system, following pathway 1 of Figure 1. We obtain a polymer made of individual metal-citrate complexes immobilized in a rigid polyester network.

However, at this stage of the preparation, two different behaviors are observed depending on the amounts of CA and EG used. These amounts are crucial parameters because they govern the distance between the cations in the polymeric network. When cations are well distributed and are very close to each other (i.e., small amounts of both CA and EG, CA/M = 1 and EG/CA = 1), polymerization, decomposition of the organic matrix, and chemical reaction occur almost simultaneously at low temperature and in a short time. The heat flow generated from the organic matrix decomposition is enough to locally synthesize the oxide. XRD and TGA experiments will confirm the formation of LLTO as it will be seen later in this paper. As soon as the cations are far away from each other (i.e., high amounts of CA and EG), they have to diffuse before interacting. More energy is then needed, and therefore a higher synthesis temperature and a longer time are required. A heating at 350 °C for 2 h in an oven is required for pyrolysis, as previously described by Vijayakumar et al.[11c] Therefore, a gray-to-black powder of cation precursors is formed at this point of the preparation. A further heating at 900 °C for 2 h is necessary to obtain a pure and crystalline phase of LLTO whatever the high value of CA/M and EG/CA molar ratios.

Figure 2 shows four pictures of the powder obtained after a first heating at 140 °C for 30 min in an oil bath and a second heating at 350 °C for 2 h in an oven. The white color of Figure 2a suggests that the chemical reaction is complete and that LLTO is formed. On the other hand, the gray and black colors of the powders shown in Figure 2b−d indicate that these powders contain carbon and that the chemical reaction is not yet complete.

Figure 3 shows the TGA curves obtained in air from the powders shown in Figure 2, in the temperature range from

(12) Xu, Y.; Yuan, X.; Huang, G.; Long, H. *Mater. Chem. Phys.* **2005**, *90*, 333.

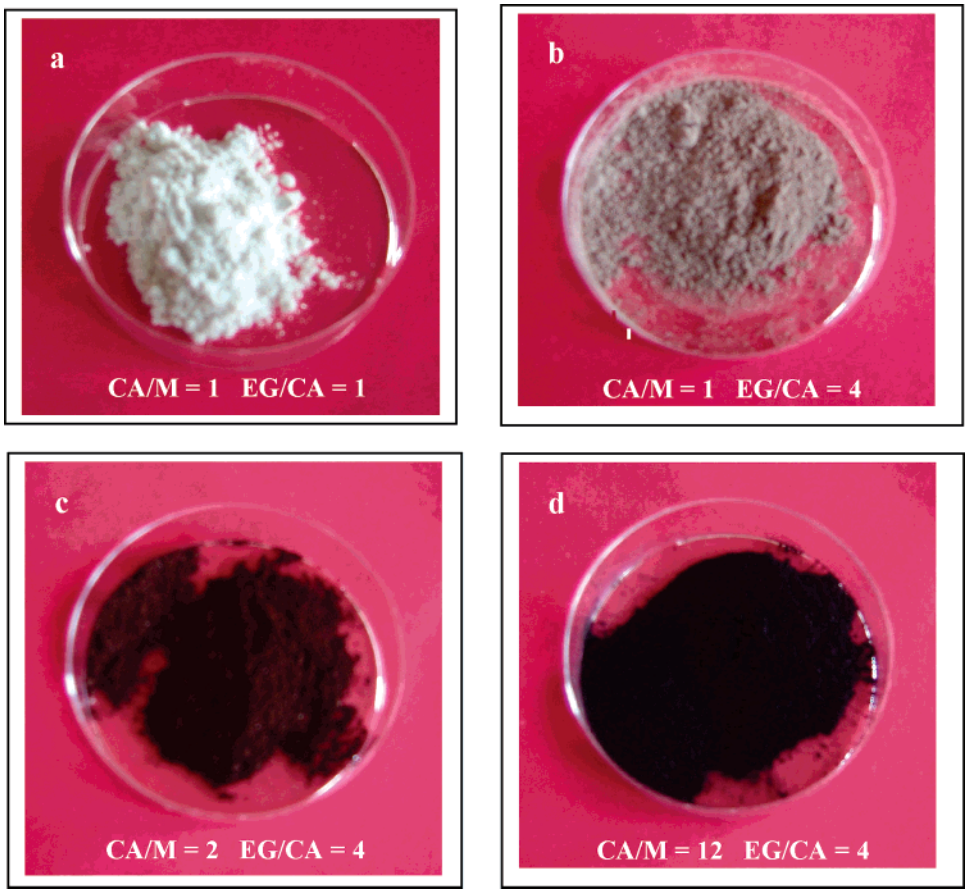

Figure 2. Powders obtained after a first heating at 140 °C for 30 min in an oil bath followed by a second heating at 350 °C for 2 h in an oven. Different ratios of CA/M and EG/CA have been used.

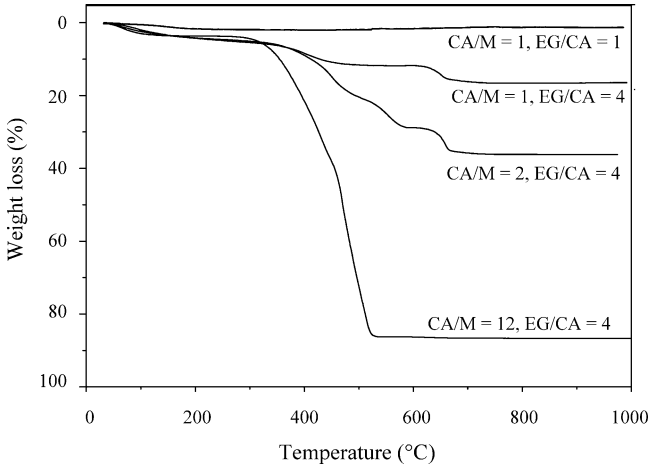

Figure 3. TGA, performed in air at 5 °C min^{-1}, of powders obtained after a first heating at 140 °C for 30 min in an oil bath followed by a second heating at 350 °C for 2 h in an oven. Different ratios of CA/M and EG/CA have been used.

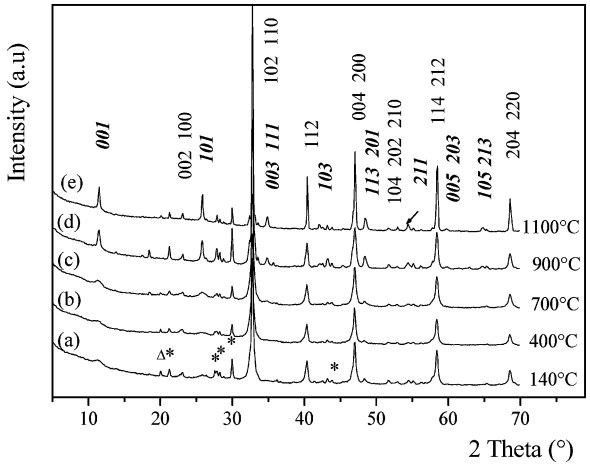

Figure 4. XRD patterns recorded at room temperature of a powder sample (CA/M = 1, EG/CA = 1) after heating at 140 °C for 30 min (pattern a). The diffraction diagrams b−e are recorded at RT after further heat treatment of the powder in the temperature range from 400 °C to 1100 °C. LLTO reflections are labeled by their Miller indices, *hkl* (in italics for superstructure peaks), calculated from ref 15. *: $La_2Ti_2O_7$ (JCPDS-ICCD # 081-1066), △: $Li_2Ti_3O_7$ (JCPDS-ICCD # 034-0393).

30 to 1000 °C. For small amounts of CA and EG (i.e., CA/M = 1 and EG/CA = 1), a small weight loss of 2% is observed around 100 °C which is mostly due to water desorption. No further weight loss occurs confirming that the polymer has been already decomposed at this temperature. For the other amounts of CA and EG, a weight loss varying from 10% to 85% is observed in the temperature range from 300 °C to 700 °C. This weight loss is due to the degradation of the polymer, converting the organic compounds into CO_2 and H_2O.

The main point of this study is the finding that LLTO can be prepared at a very low temperature (i.e., 140 °C). To confirm this result, an XRD experiment has been performed on the powder obtained with the molar ratios CA/M = 1 and EG/CA = 1 after heating at 140 °C for 30 min by following pathway 1 of Figure 1. The XRD pattern (Figure 4a) clearly reveals that LLTO is formed. However, some impurities, $Li_2Ti_3O_7$ (JCPDS-ICCD # 034-0393) and La_2-

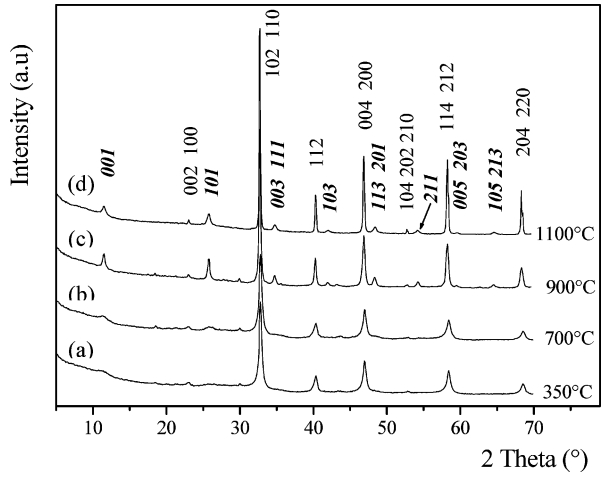

Figure 5. XRD patterns recorded at room temperature of a powder sample (CA/M = 1, EG/CA = 1) after heating at 120 °C for 20 min followed by a heat treatment at 350 °C for 2 h (pattern a). The diffraction diagrams b−d are recorded at RT after further heat treatments of the powder in the temperature range from 400 °C to 1100 °C. LLTO reflections are labeled by their Miller indices, *hkl* (in italics for superstructure peaks), calculated from ref 15.

Ti_2O_7 (JCPDS-ICCD # 081-1066), marked as triangle and asterisks, respectively, are present in this compound. XRD patterns, recorded after further heating of the powder in the temperature range from 400 °C to 1100 °C, show that these impurities do not disappear with increasing temperature (patterns 4b−4e). This result means that these impurities are thermally stable.

Synthesis of the Pure Phase of $Li_{0.30}La_{0.56}TiO_3$. To obtain the pure phase of LLTO, the synthesis method has to be improved. Because the above study has clearly shown that low molar ratios of CA/M and EG/CA (i.e., CA/M = 1 and EG/CA = 1) allowed us to obtain LLTO at low temperature, we kept constant these ratios and we tried to improve the synthesis method to avoid the formation of impurities. Therefore, pathway 2 of Figure 1 has been followed. After esterification at 60 °C for 1 h and at 90 °C for 30 min, a heating at only 120 °C for 20 min in the oil bath is performed with magnetic stirring. A gray powder is obtained indicating that polymerization and partial decomposition of the organic compounds occurred. At this temperature, LLTO is not yet formed. The powder is then heated at 350 °C for 2 h in an oven. A white powder is obtained. Figure 5a shows the XRD pattern of this white powder, recorded at room temperature. We observe that LLTO is formed and that the amount of impurities is very low but that the phase is not perfectly crystallized.

It can be postulated that a low temperature (i.e., 120 °C) limits the kinetics of the polymerization process and then favors a better uniform distribution of the cations through the polymeric resin by controlling the viscosity of the solution. However, the decomposition of the organic compound is limited at this low temperature and then the heat flow generated from the organic matrix decomposition is not important enough to locally synthesize the oxide. A gray powder of precursor with cations uniformly distributed is then obtained. Because of this uniform distribution of cations, a further increase of temperature up to 350 °C for 2 h promotes the chemical reaction between the precursors and favors the formation of LLTO by preventing the formation of impurities, as seen in the XRD spectra of Figure 5a. On the other hand, a higher temperature (i.e., 140 °C as used when pathway 1 of Figure 1 is followed) increases both the kinetics of the polymerization process and the complete decomposition of the organic matrix. The heat flow generated from this decomposition is then important enough to locally promote the chemical reaction of LLTO. Because the polymerization occurs more rapidly, the viscosity is more important and therefore the cations are not so well distributed through the polymeric resin. Impurities are then more easily formed (Figure 4a). The viscosity of the solution is then very important and controls the cation distribution into the polymer matrix and consequently the formation of impurities. When these impurities are thermally stable, as it is the case for $Li_2Ti_3O_7$ and $La_2Ti_2O_7$, they cannot disappear by further heating of the powder. We have clearly demonstrated that a careful control of the polymerization temperature, after esterification, can minimize the formation of impurities.

To improve the crystallinity of the oxide, further heat treatments of the powder have been performed. After heat treatments, XRD patterns have been recorded at RT (Figure 5). The patterns 5b−d show that an increase of the temperature leads to a narrowing of all the diffraction lines. However, all the diffraction lines do not behave similarly. A drastic narrowing of the superstructure lines (*hkl* with $l = 2n + 1$) is observed above 900 °C (patterns 5c and 5d). This phenomenon is also observed in Figure 4 (patterns 4d and 4e). This sudden narrowing of the superstructure lines can be explained by the thermal diffusion of the La^{3+} ions above this temperature, as previously pointed out by Harada et al.[13] and by Bohnke et al.[14] This explanation agrees well with previous results that appeared in the literature on LLTO prepared under different synthesis conditions. First, when LLTO is prepared by the conventional solid-state reaction followed by a slow cooling to room temperature, XRD patterns show that superstructure lines, slightly broader than the other diffraction lines, are present.[15] The high-temperature synthesis (i.e., 1150 °C) leads to a complete disordering of the La^{3+} ions in the structure by thermal La^{3+} diffusion. A slow cooling to RT favors some ordering of the La^{3+} ions in the A-cages of the perovskite structure. LLTO is then structurally well described either in the *P4*/*mmm*[15] or *Cmmm*[16] space groups. In these structural models, the La^{3+} ions are unequally distributed in the two adjacent A-cages of the perovskite network along the *c* direction. This unequal distribution of La^{3+} ions is responsible for the doubling of the *c* axis parameter and for the presence of the superstructure lines. This implies the existence in the perovskite structure of La^{3+}-rich layers and La^{3+}-poor layers in the (*a*, *b*) planes of the structure. Because the stacking of these layers are not perfectly ordered in the *c*-direction, the superstructure lines

(13) Harada, Y.; Ishigaki, T.; Kawai, H.; Kuwano, J. *Solid State Ionics* **1998**, *108*, 407.
(14) Bohnke, O.; Duroy, H.; Fourquet, J.-L.; Ronchetti, S.; Mazza, D. *Solid State Ionics* **2002**, *149*, 217.
(15) Fourquet, J.-L.; Duroy, H.; Crosnier-Lopez, M.-P. *J. Solid State Chem.* **1996**, *127*, 283.
(16) Inaguma, Y.; Katsumata, T.; Itoh, M.; Morii, Y. *J. Solid State Chem.* **2002**, *166*, 67.

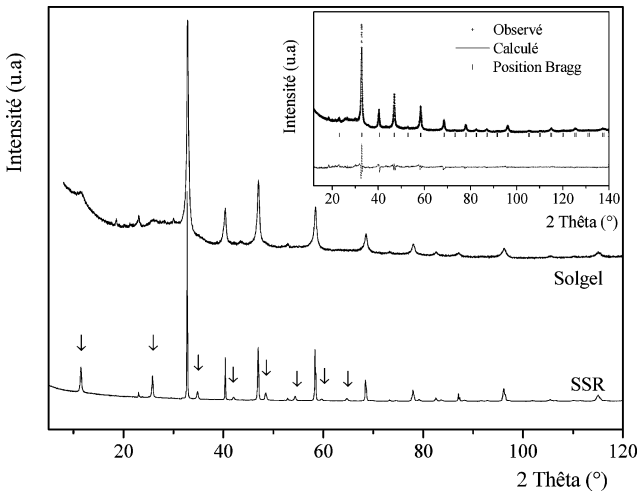

Figure 6. Powder XRD patterns of $Li_{0.30}La_{0.56}TiO_3$ obtained by solid-state reaction (SSR) or Pechini-type in-situ polymerizable method at 350 °C for 2 h (pathway 2 of Figure 1) (↓: superstructure lines). A Rietveld refinement, with cubic symmetry, using HighScore Plus software, is shown in the insert.

are slightly broader than the other diffraction lines (*hkl* with $l = 2n$). Second, when LLTO is prepared at high temperature and is quenched in liquid N_2, the complete disordering of the La^{3+} ions that occurs at high temperature cannot be retained by quenching. Despite this fast cooling, La^{3+}-rich layers and La^{3+}-poor layers are formed, owing to the very fast disordering/ordering La^{3+} ion process between their two unequivalent positions. Therefore, the superstructure lines are always present in the XRD patterns.[14] However, they are very broad suggesting a great disorder in the stacking of these two layers. Finally, when the oxide is prepared at low temperature by the polymerizable method, La^{3+}-rich layers and La^{3+}-poor layers are present, but the stacking cannot be ordered during the heat treatment at 350 °C since La^{3+} thermal diffusion cannot occur. This leads to very broad superstructure lines as in the quenched samples. By increasing the temperature, the La^{3+} thermal diffusion that occurs around 900 °C favors the ordering of the two different layers. Consequently, the superstructure lines suddenly narrow.

Nanostructure of the Pure Phase of $Li_{0.30}La_{0.56}TiO_3$. Slow-scan powder X-ray diffraction patterns have been recorded at room temperature for LLTO obtained by either the herein used low-temperature synthesis procedure route (pathway 2 of Figure 1) or the classical high-temperature solid-state chemical reaction route. Figure 6 shows the two spectra indicating the formation of the pure phase of LLTO at temperature as low as 350 °C. A very small amount of $La_2Ti_2O_7$ can be detected in both compounds. The main difference in these diffraction diagrams is the broadness of all the diffraction lines of LLTO obtained by the polymerizable method. As described above, the superstructure lines (*hkl* with $l = 2n + 1$) are broader than the other diffraction lines (*hkl* with $l = 2n$).

The determination of the grain size has been carried out by the analysis of the slow-scan XRD pattern of the powder. Generally, this method provides a powerful and nondestructive way for the analysis of the microstructure of materials, via the analysis of diffraction-line broadening. However, this method of determining crystallite size is not trivial, and different and sometimes conflicting procedures appeared in the literature. From a general point of view, the broadening of diffraction lines occurs for two principal reasons: instrumental effects and physical origins (for the most current reviews on this topic, consult the monograph of Snyder et al.[17] and the more recent one of Mittermeijer and Scardi[18]). The broadening due to physical origins can be roughly divided into diffraction-order-independent (size) broadening and diffraction-order-dependent (strain) broadening in reciprocal space.

We used, in a first approximation, the Scherrer relationship (eq 1) to estimate the grain size. However, several factors can affect the correctness of the result (an error as high as 70% can be attained). The factors affecting the estimation include the choice of the Bragg peaks and the mathematic function used to extract the full width at half maximum (fwhm) values. Furthermore, a tendency of an underestimation of the grain size is observed by neglecting the microstrain components in the Scherrer equation. As reported by Zhang[19] on nanocrystalline Al, the estimated crystallite size is strongly dependent on the choice of the Bragg peaks. These authors clearly showed that the choice of the more intense line, as generally made in most of the papers, is not the best one. To minimize the role of these factors and to limit the error, we used some reflections to estimate the grain size. An average crystallite size of 32 nm has then been determined. We recall that, in this procedure, the strain-broadening effect is neglected.

To go further in this study, two types of approaches are available: the phenomenological "top−bottom" approaches, such as integral−breadth methods, and the Fourier methods. In a reference work, Balzar et al.[20] compared the three most famous methods: the model assuming a log-normal size distribution of spherical crystallites, the Warren-Averbach analysis, and the Rietveld refinement. For our particular case, we choose the Rietveld method to estimate the size and the strain parameters. By this method, a pseudo-Voigt function is used and both Lorentzian and Gaussian contributions were refined to obtain L and e values, as described in the Experimental Section.

As discussed above, the obtained compound is not cubic because of the unequal distribution of La^{3+} ions into the two A-sites and because of the disordered stacking of the layers. The very broad diffraction lines related to this phenomenon were really difficult to be taken into account for a correct refinement. In a first approximation, we assumed that this compound adopts an ideal cubic symmetry. A Rietveld refinement was then performed on the space group $Pm3\,m$ (ICSD: 92238): $a = 3.8819$ (2) Å, $R_p = 5.86$, and $R_{wp} = 7.75$. The average crystallite size (coherence length) is 23 nm with a microstrain parameter of 0.16%. When using the

(17) Snyder, R. L.; Fiala, J.; Bunge, H. J. *Defect and Microstructure Analysis by Diffraction*; Oxford University Press: IUCr/Oxford, 1999.
(18) Mittemeijer, E. J.; Scardi, P. *Diffraction Analysis of the Microstructure of Materials*; Springer: Berlin, 2004.
(19) Zhang, Z.; Zhou, F., Lavernia, E. J. *Metall. Mater. Trans. A* **2003**, *34A*, 1349.
(20) Balzar, D.; Audebrach, N.; Daymond, M. R.; Fitch, A.; Hewat, A.; Langford, J. L.; Le Bail, A.; Louër, D.; Masson, O.; McCowan, C. N.; Popa, N. C.; Stephens, P. W.; Toby, B. H. *J. Appl. Crystallogr.* **2004**, *37*, 911.

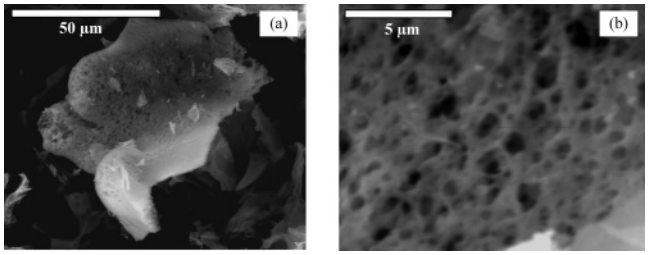

Figure 7. SEM micrographs of $Li_{0.30}La_{0.56}TiO_3$ prepared by the Pechini-type in-situ polymerizable method at 350 °C for 2 h (pathway 2 of Figure 1).

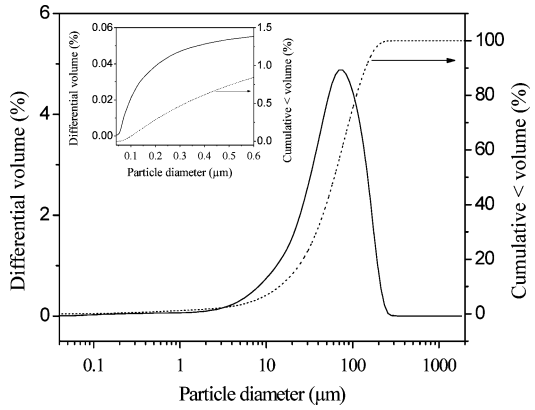

Figure 8. Laser granulometry curve obtained from $Li_{0.30}La_{0.56}TiO_3$ prepared by the Pechini-type in-situ polymerizable method at 350 °C for 2 h (pathway 2 of Figure 1). Differential (solid line) and cumulative (dashed line) volume percentage particle size distribution are plotted on the left and the right axis, respectively.

superstructure lines as a "second phase", as suggested by Fourquet et al.,[15] the Rietveld refinement with a *P*4/*mmm* space group (ICSD: 82671) leads to $a = 3.8817(9)$ Å, $c = 7.7700(4)$ Å, $R_p = 7.39$, and $R_{wp} = 10.31$. The reliability factors are slightly higher than in the cubic assumption. An average crystallite size of 26 nm with a microstrain parameter of 0.10%, close to the previous values, is found. However, the *U*, *V*, and *W* values for the superstructure lines are not determined with good accuracy. These values of 23 and 26 nm are in very good agreement with the previous one determined with the Scherrer equation (32 nm). Furthermore, the small values of strain parameter of 0.16% and 0.10% obtained in both assumptions allowed us to validate the use of the Scherrer relationship. However, the use of Rietveld refinement for microstructural analysis is always difficult and complicated, and the results obtained have to be taken with much care, as discussed in a recent paper.[20] Therefore, we used electronic microscopic techniques to characterize the microstructure of LLTO and to confirm these previous results.

SEM micrographs of LLTO obtained at 350 °C are presented in Figure 7. Figure 7a shows the presence of aggregates. This result is confirmed by laser granulometry experiment, shown in Figure 8, which reveals the existence of aggregates of 5−200 μm in size. Figure 7b shows the macroporous character of the powder with a pore size around 1 μm. At the present time, macroporous materials also deserve much attention because of their possible use in various electrochemical applications, such as sensors or batteries. It is in this context that recently Dokko et al. reported the preparation of three-dimensionally ordered macroporous $Li_{0.35}La_{0.55}TiO_3$ membrane using colloidal crystal templating method combined with sol−gel process.[21] The low-temperature synthesis used in our study may also offer some interesting way to prepare such a macroporous membrane.

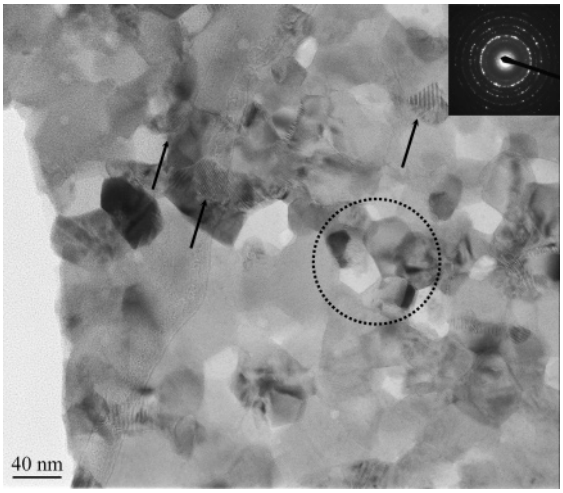

Figure 9. TEM image of $Li_{0.30}La_{0.56}TiO_3$ prepared by the Pechini-type in-situ polymerizable method at 350 °C for 2 h (pathway 2 of Figure 1).

Figure 9 shows a low-resolution TEM image revealing small grains of 20−30 nm size and presenting faceted borders, as shown in the black circle. The crystallinity of the sample is evidenced by the rings with sharp spots of the corresponding selected area diffraction pattern (at the right top) as well as by the presence of fringes (black arrows). The powder is not perfectly crystallized owing to the low-temperature process used. However, these observations confirm the nanostructure of LLTO powder. The presence of these nanoparticles are then able to explain the broadness of the diffraction lines observed in the XRD pattern of Figure 6.

Conclusion

We have reported the detailed procedure used to prepare nanosized fast ionic lithium conductor $Li_{0.30}La_{0.56}TiO_3$. The CA/M = 1 and EG/CA = 1 molar ratios are found to be the best values to obtain the formation of the oxide at very low temperature. Furthermore, the pyrolysis temperature is a crucial parameter to prevent the formation of the thermally stable impurities: $Li_2Ti_3O_7$ and $La_2Ti_2O_7$. Indeed, to prevent the formation of these impurities, it is necessary to obtain a uniform distribution of the cations in the polymer network. This can be achieved by slowing down the kinetics of the polymerization process that controls the viscosity of the solution. By adjusting both the CA/M and EG/CA molar ratios and the pyrolysis temperature, it is possible to obtain a pure phase of LLTO. This phase is made of crystallites of 20−30 nm size as determined by the analysis of the width of the XRD lines and by TEM. This phase shows a macroporous character that can offer some advantages for

(21) Dokko, K.; Akutagawa, N.; Isshiki, Y.; Hoshina, K.; Kanamura, K. *Solid State Ionics* **2005**, *176*, 2345.

particular electrochemical applications. To perform conductivity, the nanopowder has to be sintered under charge to obtain a dense pellet without increasing the grain size. Such densification is on the way to determine the conductivity and the influence of the grain size on the ionic mobility.

Acknowledgment. We thank A. Lebail for helpful discussions about microstructural analysis using XRD, and we thank T. Dortmann (PANalytical) for help in use of the X'Pert HighScore Plus software.

CM060605F